

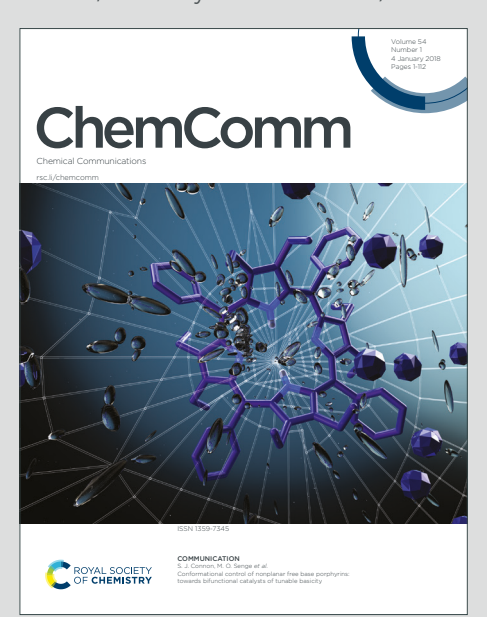
View Article Online
View Journal

ChemComm

Chemical Communications

Accepted Manuscript

This article can be cited before page numbers have been issued, to do this please use: U. Shivpuje, M. Ahmad, N. J. Roy and P. Talukdar, *Chem. Commun.*, 2025, DOI: 10.1039/D5CC04105H.



This is an Accepted Manuscript, which has been through the Royal Society of Chemistry peer review process and has been accepted for publication.

Accepted Manuscripts are published online shortly after acceptance, before technical editing, formatting and proof reading. Using this free service, authors can make their results available to the community, in citable form, before we publish the edited article. We will replace this Accepted Manuscript with the edited and formatted Advance Article as soon as it is available.

You can find more information about Accepted Manuscripts in the <u>Information for Authors</u>.

Please note that technical editing may introduce minor changes to the text and/or graphics, which may alter content. The journal's standard <u>Terms & Conditions</u> and the <u>Ethical guidelines</u> still apply. In no event shall the Royal Society of Chemistry be held responsible for any errors or omissions in this Accepted Manuscript or any consequences arising from the use of any information it contains.



nemComm Accepted Manuscrip

View Article Online DOI: 10.1039/D5CC04105H

COMMUNICATION

Ligand-responsive ON-OFF anion transport using copper-caged acylhydrazone transporters

\Received 00th January 20xx, Accepted 00th January 20xx Umesh Shivpuje,^a Manzoor Ahmad,^{a,b} Naveen J. Roy^a and Pinaki Talukdar*^a

DOI: 10.1039/x0xx000000x

Reversibly gated stimuli-responsive anion transport utilizing acylhydrazone-based transporters is reported. Acylhydrazone-copper complexation makes hydrazone protons unavailable for binding and transport, whilst decomplexation using Na₂EDTA activates the ion transport.

Ion transport across bilayer membranes, facilitated by ion channels, carriers, and ion pumps, is vital for biological functions.1 Malfunctioning of these systems could result in severe diseases like cystic fibrosis (channelopathies).^{2, 3} Artificial ion transport systems in the form of ion channels and ion carriers have emerged as an important class of compounds that promise therapeutic applications for treating channelopathies.4 Moreover, chloride transport by these systems is known to induce chloride-mediated apoptosis inside the cancer cells, opening up a new avenue to combat cancer.5 However, controlled spatiotemporal activation is vital for target-specific applications, as classical transporters are known to affect healthy cells as well. Stimulus-responsive ion transport systems controlled by external stimuli, such as light, ligands, voltage, pH, enzymes, and redox switching, are rare.⁶ Examples include gated light-responsive systems based azobenzene⁷ and stilbene,⁸ and irreversibly gated systems that provide effective ON-OFF control for ion transport. Responsive systems whose activity is controlled through the input of multiple stimuli remain rare. These provide better ON-OFF control compared to light-responsive ones, which exhibit background transport activity arising from incomplete photoconversion. Our lab has reported reversibly gated systems based acylhydrazone9 and phenylhydrazone¹⁰ photoswitches. In 2020, a foldamer-based reversibly gated ion channel was reported with transmembrane ion transport controlled chemically using Cu(II) ion and EDTA.¹¹ However, the

use of complex foldamer molecules presents a challenge for the practical application of the system.

Herein, we report a similar reversibly gated ion transporter utilizing copper(II) and Na₂EDTA as an external stimulus employing simpler acylhydrazone copper complexes. Acylhydrazone-based compounds are known to exhibit ion binding properties like heteroditopic ion pair binding. They also possess excellent ion transport properties. Acylhydrazone-based ligands, upon complexation with copper ion, are known to provide -N=C-O-Cu linkage¹² by removing hydrazone protons. We, therefore, envisaged that the complexation of carefully

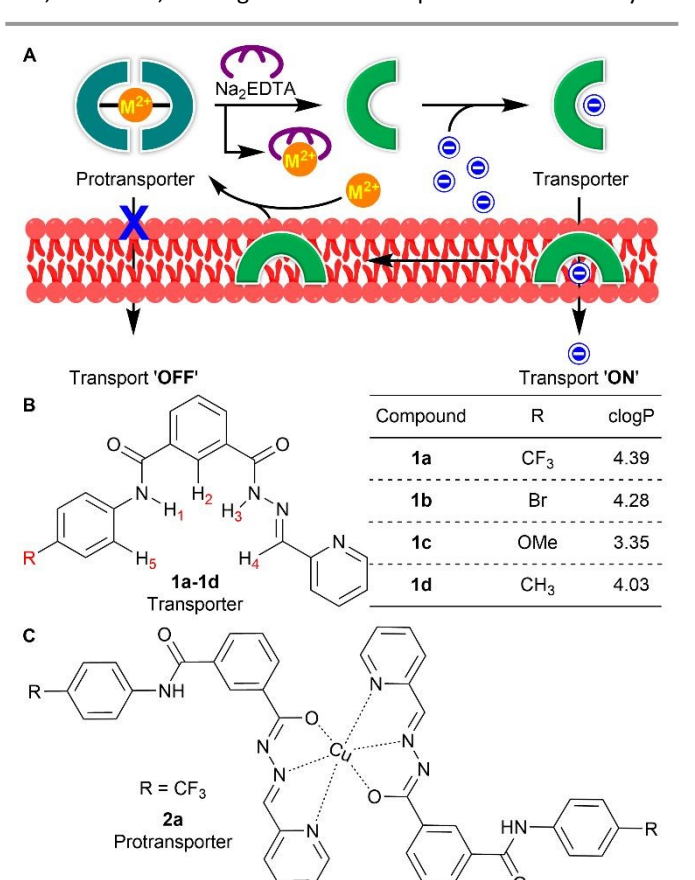


Fig. 1 Working principle of ligand-responsive ion transport (A). Molecular structures of transporters 1a-1d and their clogP values (B) and protransporter 2a, respectively (C).

^aDepartment of Chemistry, Indian Institute of Science Education and Research Pune, Dr. Homi Bhabha Road, Pashan, Pune 411008, Maharashtra, India. E-mail: ptalukdar@iiserpune.ac.in

^bPresent Address: Chemistry Research Laboratory, Mansfield Road, Oxford, OX1 3TA, UK.

Supplementary Information available: [details of any supplementary information available should be included here]. See DOI: 10.1039/x0xx00000x

COMMUNICATION **Journal Name**

designed acylhydrazone-based ion transporters with copper would make hydrazone protons unavailable for anion binding and subsequent transport (Fig. 1). Decomplexation with Na2EDTA, which would remove the copper ions, would render anion binding and transmembrane ion transport active by providing free hydrazone protons. Reversible control would be achieved using Na₂EDTA and Cu (II) as an external stimulus. We chose isophthalic biscarboxyamide hydrazone-based systems 1a-1d as active transporters, as similar molecules were found to be efficient ion transporters in our previous study. These transporters were expected to show an ion-pair transport because of an ion-pair binding in similar systems reported by Chmielewski and coworkers. 13 However, only anion transport was observed, probably because the cation bound to the transporter would be exposed to the hydrophobic domains of the lipid membrane. Meanwhile, 2a was chosen as the protransporter. Incorporating different substituents to the amide moiety was expected to fine-tune the ion transport behavior of these systems by changing their lipophilicities.

The active transporters 1a-1d were synthesized from monohydrolyzed ester 3, prepared from the reported literature.9 Subsequently, 3 was coupled with aromatic amines 4a-4d using EDC·HCI/HOBt to yield the amide derivatives 5a-5d. The reaction of 5a-5d with hydrazine hydrate, followed by coupling with 2-piconaldehyde, furnished the active transporters 1a-1d (Scheme 1). Further, compound 1b was recrystallized from methanol. The single crystal structure data are provided in the ESI (Fig. S23 and S24).

Anion-binding affinities of 1a were evaluated through 1H NMR studies. Titration of 1a with tetrabutylammonium chloride (TBACI), bromide (TBABr), iodide (TBAI) and nitrate (TBANO₃) salts in acetonitrile-d₃ led to significant downfield chemical shifts of the protons H₁, H₂, H₃, and H₄, indicating their involvement in anion binding through amide-NH₁···A⁻, ArC-H₂···A⁻, hydrazone-NH₃···A⁻, imine-CH₄···A⁻ hydrogen bonding interactions.

BindFit14 analysis furnished a 1:1 (receptor: anion) binding stoichiometry with association constant values ($K_{a(1:1)}/Cl^-$) of $(9.1 \pm 0.7) \times 10^4 \text{ M}^{-1}$, $K_{a(1:1)}/\text{Br}^- = (3.47 \pm 0.1) \times 10^3 \text{ M}^{-1}$, and $K_{a(1:1)}/I^- = 76.68 \pm 4.9 \text{ M}^{-1} \text{ and } K_{a(1:1)}/NO_3^- = 95.13 \pm 0.41 \text{ M}^{-1},$

Scheme 1. Chemical synthesis of active transporters 1a-1d and copper-caged protransporter 2a.

respectively (Fig. S3-S10). Further proof of chloride binding was obtained by high-resolution mass spectrometry (TARNAS). Peaks at m/z = 447.0842 and 449.0818 corresponding to the $[1a+Cl^{-}]$ complex were obtained in the solution state (Fig. S11).

The ion transport activity of the compounds 1a-1d was evaluated across large unilamellar vesicles (LUVs).5 8-Hydroxy pyrene-1,3,6-trisulfonic acid trisodium salt (HPTS, 1 mM) was entrapped within the vesicles containing 100 mM of NaCl and 10 mM of HEPES buffer. A pH gradient ($pH_{in} = 7.0$ and $pH_{out} =$ 7.8) was created across the lipid membrane by the addition of 0.5 M NaOH (20 µL) to the extravesicular solution. The subsequent addition of compounds 1a-1d resulted in the collapse of the pH gradient, monitored by recording the change in fluorescence intensity at λ_{em} = 510 nm (λ_{ex} = 450 nm). The activity comparison yielded a transport activity sequence of 1a > 1b > 1c > 1d (Fig. 2A). Hill analysis of dose-dependent ion transport data furnished the EC_{50} values of 5.36 μ M, 6.15 μ M, and 46.31 µM for compounds 1a, 1b, and 1c, respectively (Fig. S13-S14). Hill coefficients (n) of \sim 1 indicated that ion transport across the lipid bilayer is mediated by a 1:1 receptor: anion interaction, and this result corroborates ¹H NMR titration studies. Hill analysis of 1d could not be done due to its precipitation at higher concentrations.

Subsequently, Cl⁻ transport across EYPC-LUVs⊃lucigenin was monitored for the most active transporter 1a. Vesicles entrapping lucigenin dye were prepared in a 200 mM NaNO₃ solution, and then a Cl⁻/NO₃-gradient was created by adding NaCl (33.3 μL, 2.0 M) in the extravesicular buffer. Chloride influx was evaluated by monitoring the change in the fluorescence intensity (λ_{ex} = 455 nm and λ_{em} = 535 nm) after the addition of 1a. The dose-dependent Cl⁻ influx by 1a is shown in Fig. S17. Hill analysis furnished an EC₅₀ value of 9.34 μM with a Hill coefficient (n) of ~ 1 as obtained in the above-mentioned HPTS studies.

Mechanistically, ion transport in the lucigenin assay could occur through H+/Cl- symport, M+/Cl- symport, or Cl-/OHantiport modes. However, varying anions in the external buffer using different NaX salts (X = Cl⁻, Br⁻, OAc⁻, NO₃⁻, and ClO₄⁻) strongly affect the ion transport (Fig. 2B), and variation of extravesicular MCl salts (M = Li+, Na+, K+, Rb+, and Cs+) in lucigenin-based studies did not change the ion transport (Fig. S19). These observations ruled out M⁺/Cl⁻ symport and M⁺/H⁺ antiport, which indicated that ion transport could occur either through H+/Cl- symport or Cl-/OH- antiport mode. To get further insights, chloride efflux using 1a was monitored using a chloride ion selective electrode (ISE) in the presence and absence of either valinomycin (a highly selective K+ transporter) or monensin (an H+/K+ antiporter) with intravesicular KCl (300 mM) and extravesicular potassium gluconate (300 mM) solutions. 15 A significant enhancement in the Cl-efflux rate was observed for 1a in the presence of valinomycin, while it remained nearly unchanged with monensin. This enhanced Clefflux in the presence of valinomycin provided evidence of transporter-mediated electrogenic transport. Selective K+ transport by valinomycin complements anion transport by 1a, suggesting an antiport mechanism of transport (i.e., Cl-/ OH-). However, the lack of Cl- efflux enhancement with monensin

Journal Name COMMUNICATION

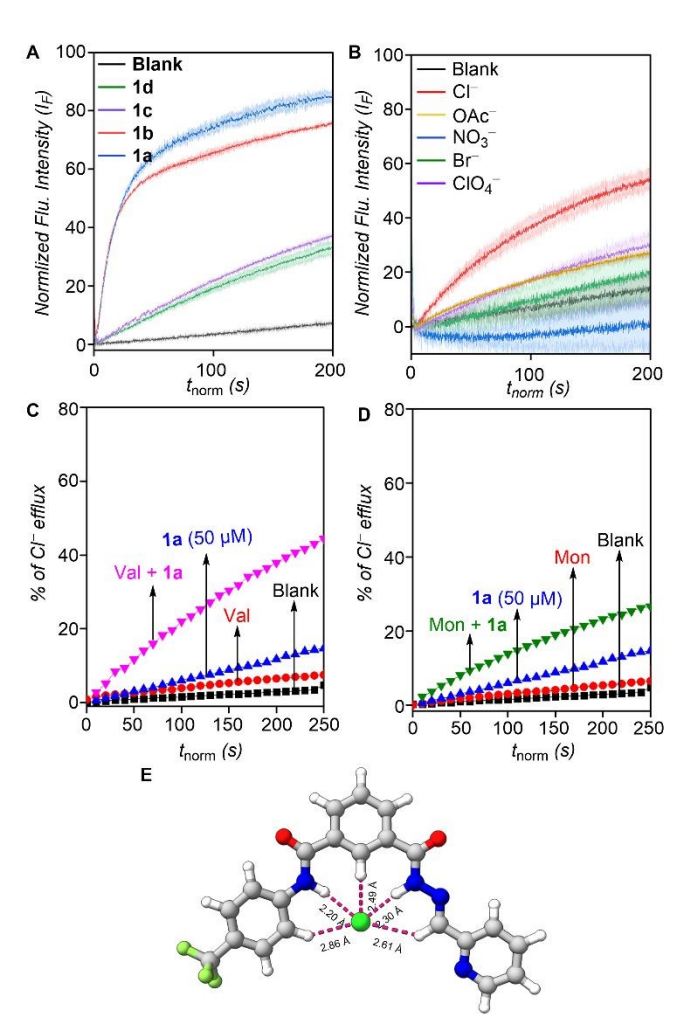


Fig. 2 Activity comparison of **1a–1d** (20.0 μM each) across EYPC–LUVs⊃HPTS (A). Anion selectivity of **1a** (3.5 μM) by varying external anions across EYPC–LUVs⊃HPTS (B). Normalized chloride efflux of **1a** in the presence and absence of valinomycin (C) and the presence and absence of monensin (D). The geometry-optimized structure of [**1a**+Cl⁻] complex (E).

rules out an H^+/Cl^- symport mechanism for **1a** (Fig. 2C, 2D, and S21).

The necessary evidence for a mobile carrier mechanism for ion transport was explored through experiments conducted in the liquid gel phase of dipalmitoylphosphatidylcholine (DPPC) large unilamellar vesicles (LUVs). 16 Inactivity at 25 °C, and restoration of activity at 45 °C, which is above the gel-liquid phase transition temperature for DPPC ($T_m = 41$ °C), is indicative of a mobile carrier process rather than transport mediated by selfassembly into an ion channel, that activity of which would be typically expected to be independent of the lipid phase (Fig. S18). Based on the experimentally determined Hill coefficient value of $n \sim 1$ the geometry-optimized structure of [1a+Cl⁻] complex was obtained first by generating the most probable conformation by using the CONFLEX 8 program¹⁷ (Fig. S25). Subsequently, the geometry optimization of the generated conformation was done by the Gaussian 09 program (see ESI) using the B3LYP functional and 6-31G(d,p)18 basis set. The geometry-optimized structure confirmed that the receptor participates in the anion recognition through amide-NH₁···Cl⁻

 $(H\cdots Cl^- = 2.20 \text{ Å})$, Hydrazone $NH_3\cdots Cl$ $(H\cdots Cl^- = 2.30 \text{ Å})$, Lighting $CH_4\cdots Cl^ (H\cdots Cl^- = 2.61 \text{ Å})$, and $Ar-CH_5\cdots Cl^-1$ $(H^{0.30}l^-) \le 2.860 \text{ Å})$ hydrogen bonding interactions (Fig. 2E and S27). The computed binding energy was found to be -45.02 kcal mol^{-1} .

The copper complexed protransporter 2a was synthesized by refluxing the best active transporter 1a with copper chloride dihydrate in methanol (Scheme 1). The broad peaks observed in the ¹H NMR spectra of compound **2a** indicate paramagnetic characteristics, which were further confirmed by EPR spectra, revealing the presence of an unpaired electron consistent with a 3d9 configuration (Fig. S2). The lack of acyl hydrazone-NH3 protons in the ¹H NMR spectrum of **2a**, along with the (Cu⁺²) 3d⁹ configuration confirmation through EPR, suggests the bonding structure of 2a is -N=C-O-Cu. Furthermore, to assess the rigidity of [Cu(1a)2], variable-temperature (VT) EPR measurements were conducted. The results showed no difference in the g value, indicating that [Cu (1a)2] remains stable from 100 K to The decomplexation of copper-hydrazone complex 2a to form 1a using Na₂EDTA was initially analyzed by ¹H NMR spectroscopy. Na₂EDTA solution in D₂O was added to a sample of 2a in DMSO-d₆, and the NMR spectrum was recorded. ¹H NMR of the copper complex was observed to be broad due to the paramagnetic characteristics of the Cu-d⁹ system. However, the addition of Na₂EDTA led to the appearance of NMR peaks, such as the hydrazine N-H3 at 12.25 ppm and the Ar C-H₅ proton at 7.5 ppm. All these changes indicate the formation of active transporter 1a (Fig. S22). The decomplexation of compound 2a was additionally confirmed through UV-Vis absorption analyses. The absorbance observed at 370 nm for compound 2a (20 µM) in MeOH: H₂O (9:1) solvent may be due to a charge transfer (CT) transition. 19 The stepwise addition of Na₂EDTA to 2a led to a hypochromic shift at 370 nm and a hyperchromic shift seen at 297 nm, indicative of the formation of 1a from 2a which was validated by the absorbance measurement of compound 1a in the same solvent at a concentration of 37 μ M (Fig. 3A). Approximately 1.4 equivalents of Na₂EDTA were required to fully decomplex compound 2a during this titration. This analysis also revealed a rapid decoupling of the copper hydrazone complex upon addition of Na₂EDTA. The quick disappearance of the 370 nm peak associated with copper ligand interaction confirmed the efficacy of the ligand exchange process. After analyzing the decomplexation of 2a in the solution phase, responsive ion transport studies were performed in HPTS-based vesicular experiments, as mentioned earlier. Compound 2a at 10 μM concentration did not show any ion transport activity, while transporter 1a at the same concentration displayed maximal activity. The significant improvement in fluorescent intensity after decomplexation of 2a with Na₂EDTA, suggests the formation of 1a (Fig. 3B). Additionally, reversible ON-OFF ion transport assay was conducted by utilizing Na₂EDTA and copper as external triggers (Fig. 3C). When Na₂EDTA (1.4 eq.) was added to the solution of 2a (20 μM in DMSO) to chelate Cu(n), it resulted in a marked enhancement in ion transport, while the addition of copper chloride dihydrate (1.1 eq.) to the activated solution halted the ion transport activity. This ON-OFF ion transport behavior using two distinct stimuli was successfully maintained across multiple cycles with minimal loss

Journal Name

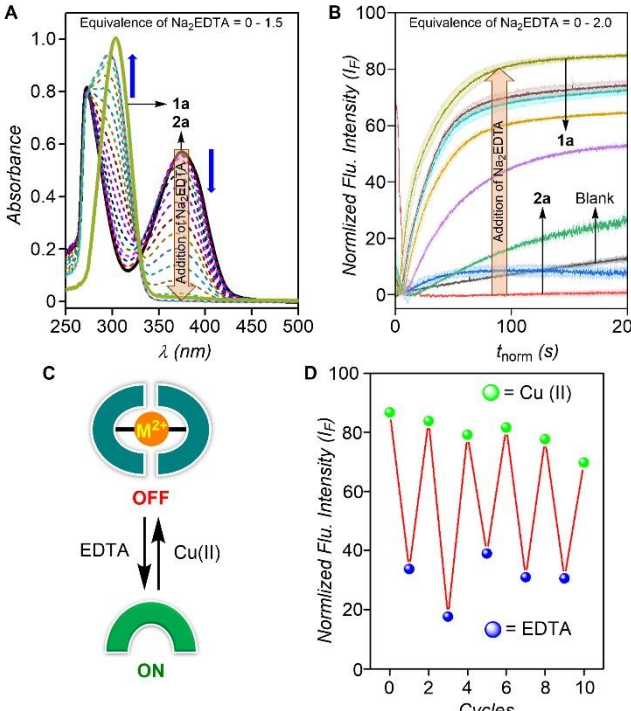


Fig. 3 UV titration compound 2a is represented with the addition of Na_2 EDTA (A). Ion transport activity of 2a (10 μ M) upon addition of Na_2 EDTA across EYPC–LUVs \Box HPTS. (B). Schematic representation of OFF-ON responsive behavior (C). ON-OFF ion transport activity of 2a upon addition of Na_2 EDTA and Cu (II) ions (D).

in performance (Fig. 3D).

This article is licensed under a Creative Commons Attribution-NonCommercial 3.0 Unported Licence

Open Access Article. Published on 06 2025. Downloaded on 09/11/25 12:56:29.

In conclusion, we have developed reversibly-gated stimuliresponsive anion transporters based on acylhydrazones frameworks, exemplified by compound 1a. Coordination of 1a with Cu(II) ions affords a 2:1 stoichiometric complex 2a, which remains inactive toward anion transport owing to the sequestration of the hydrazone proton essential for anion recognition. Subsequent decomplexation with Na₂EDTA restores the free hydrazone form 1a, thereby reinstating its anion transport activity. Reversible ON-OFF switching of ion transport was reproducibly achieved over multiple cycles by the alternate addition of Cu(II) ions and Na₂EDTA as external chemical stimuli. This study highlights the utility of metal-ligand coordination as a dynamic regulatory element in the design of stimuli-responsive molecular systems capable of controlled chloride transport. The present strategy is anticipated to be transferable to congeners 1b-1d and other appropriately designed ligands, providing a versatile platform for the development of bioinspired materials with potential therapeutic relevance.

PT acknowledges the financial support from the Anusandhan National Research Foundation (ANRF) (Project No. CRG/2022/001640) and the Indian Institute of Science Education and Research (IISER), Pune. US thanks the University Grants Commission (UGC), Govt of India, for a fellowship (UGC-NFOBC). MA thanks the University Grants Commission (UGC), Govt of India, for a fellowship. NR acknowledges the Council of Scientific and Industrial Research (CSIR), Govt of India, for a research fellowship.

Data availability

View Article Online DOI: 10.1039/D5CC04105H

All supporting data for this article are provided in the ESI.

Crystallographic data have been deposited at the Cambridge

Crystallographic Data Centre (CCDC) with ID 2473653 for **1b** and

can be obtained from

https://www.ccdc.cam.ac.uk/structures/.

Conflicts of interest

"There are no conflicts to declare".

Notes and references

- T. J. Jentsch, C. A. Hübner and J. C. Fuhrmann, Nat. Cell Biol., 2004, 6, 1039-1047.
- D. C. Gadsby, P. Vergani and L. Csanády, Nature, 2006, 440, 477-483.
- G. Bernard and M. I. Shevell, *Pediatr. Neurol.*, 2008, 38, 73-85.
- 4. R. Planells-Cases and T. J. Jentsch, *Biochim. Biophys. Acta Mol. Basis Dis.*, 2009, **1792**, 173-189.
- T. Saha, M. S. Hossain, D. Saha, M. Lahiri and P. Talukdar, J. Am. Chem. Soc., 2016, 138, 7558-7567.
- S. Chattopadhayay and P. Talukdar, Curr Opin Chem Biol., 2025, 85, 102582.
- W. Szymański, J. M. Beierle, H. A. V. Kistemaker, W. A. Velema and B. L. Feringa, *Chem. Rev.*, 2013, **113**, 6114-6178.
- S. J. Wezenberg, L.-J. Chen, J. E. Bos, B. L. Feringa, E. N. W. Howe, X. Wu, M. A. Siegler and P. A. Gale, *J. Am. Chem. Soc.*, 2022. 144, 331-338.
- 9. M. Ahmad, S. Chattopadhayay, D. Mondal, T. Vijayakanth and P. Talukdar, *Org. Lett.*, 2021, **23**, 7319-7324.
- 10. M. Ahmad, D. Mondal, N. J. Roy, T. Vijayakanth and P. Talukdar, *ChemPhotoChem*, 2022, **6**, e202200002.
- A. D. Peters, S. Borsley, F. della Sala, D. F. Cairns-Gibson, M. Leonidou, J. Clayden, G. F. S. Whitehead, I. J. Vitórica-Yrezábal, E. Takano, J. Burthem, S. L. Cockroft and S. J. Webb, Chem. Sci., 2020, 11, 7023-7030.
- 12. S. Mondal, S. Naskar, A. K. Dey, E. Sinn, C. Eribal, S. R. Herron and S. K. Chattopadhyay, *Inorganica Chim. Acta*, 2013, **398**, 98-105.
- Z. Kokan and M. J. Chmielewski, J. Am. Chem. Soc., 2018, 140, 16010-16014.
- 14. P. Thordarson, Chem. Soc. Rev., 2011, 40, 1305-1323.
- 15. L. Rose and A. T. A. Jenkins, *Bioelectrochemistry*, 2007, **70**, 387-393.
- A. Kerckhoffs and M. J. Langton, Chem. Sci., 2020, 11, 6325-6331.
- 17. a) H. Goto and E. Osawa, *J. Am. Chem. Soc.*, 1889, **111**, 8950-8951. b) H. Goto, S. Obata, N. Nakayama, K. Ohta, CONFLEX 8; CONFLEX Corporation: Tokyo, Japan, 2017.
- 18. A. D. Becke, J. Chem. Phys., 1993, 98, 5648-5652.
- 19. A. K. Patel, R. N. Jadeja, H. Roy, R. N. Patel, S. K. Patel, R. J. Butcher, M. Cortijo and S. Herrero, *Polyhedron*, 2020, **186**, 114624.

ChemComm Accepted Manuscript

View Article Online

DOI: 10.1039/D5CC04105H

Data Availability Statement

Il supporting data for this article are provided in the ESI. Crystallographic data have been deposited at the Cambridge Crystallographic Data Centre (CCDC) with ID 2473653 for 1b and can be obtained from https://www.ccdc.cam.ac.uk/structures/.